



**HAL**  
open science

**High throughput micropatterning of interspersed cell arrays using capillary assembly** This content has been downloaded from IOPscience. Please scroll down to see the full text. **High throughput micropatterning of interspersed cell arrays using capillary assembly**

François-Damien Delapierre, Guillaume Mottet, Vélain Taniga, Julie Boisselier, Jean-Louis Viovy, Laurent Malaquin

► **To cite this version:**

François-Damien Delapierre, Guillaume Mottet, Vélain Taniga, Julie Boisselier, Jean-Louis Viovy, et al.. High throughput micropatterning of interspersed cell arrays using capillary assembly This content has been downloaded from IOPscience. Please scroll down to see the full text. High throughput micropatterning of interspersed cell arrays using capillary assembly. *Biofabrication*, 2017, 9 (1), pp.015015. 10.1088/1758-5090/aa5852 . hal-01562500

**HAL Id: hal-01562500**

**<https://laas.hal.science/hal-01562500v1>**

Submitted on 15 Jul 2017

**HAL** is a multi-disciplinary open access archive for the deposit and dissemination of scientific research documents, whether they are published or not. The documents may come from teaching and research institutions in France or abroad, or from public or private research centers.

L'archive ouverte pluridisciplinaire **HAL**, est destinée au dépôt et à la diffusion de documents scientifiques de niveau recherche, publiés ou non, émanant des établissements d'enseignement et de recherche français ou étrangers, des laboratoires publics ou privés.

## High throughput micropatterning of interspersed cell arrays using capillary assembly

This content has been downloaded from IOPscience. Please scroll down to see the full text.

### Download details:

IP Address: 152.3.102.242

This content was downloaded on 12/01/2017 at 19:55

Manuscript version: Accepted Manuscript

Delapierre et al

To cite this article before publication: Delapierre et al, 2017, Biofabrication, at press:

<http://dx.doi.org/10.1088/1758-5090/aa5852>

This Accepted Manuscript is copyright Copyright 2017 IOP Publishing Ltd

During the embargo period (the 12 month period from the publication of the Version of Record of this article), the Accepted Manuscript is fully protected by copyright and cannot be reused or reposted elsewhere.

As the Version of Record of this article is going to be / has been published on a subscription basis, this Accepted Manuscript is available for reuse under a CC BY-NC-ND 3.0 licence after a 12 month embargo period.

After the embargo period, everyone is permitted to use all or part of the original content in this article for non-commercial purposes, provided that they adhere to all the terms of the licence <https://creativecommons.org/licences/by-nc-nd/3.0>

Although reasonable endeavours have been taken to obtain all necessary permissions from third parties to include their copyrighted content within this article, their full citation and copyright line may not be present in this Accepted Manuscript version. Before using any content from this article, please refer to the Version of Record on IOPscience once published for full citation and copyright details, as permissions will likely be required. All third party content is fully copyright protected, unless specifically stated otherwise in the figure caption in the Version of Record.

When available, you can view the Version of Record for this article at:

<http://iopscience.iop.org/article/10.1088/1758-5090/aa5852>

# High throughput micropatterning of interspersed cell arrays using capillary assembly

François-Damien Delapierre,<sup>a</sup> Guillaume Mottet,<sup>a</sup> Vélán Taniga,<sup>a</sup> Julie Boisselier,<sup>a</sup> Jean-Louis Viovy<sup>a</sup> and Laurent Malaquin<sup>a,b</sup>

A novel technology is reported to immobilize different types of particles or cells on a surface at predefined positions with a micrometric precision. The process uses capillary assembly on arrays of crescent-shaped structures with different orientations. Sequential assemblies in different substrate orientations with different types of particles allow for the creation of imbricated and multiplexed arrays. In this work up to four different types of particles were deterministically localized on a surface. Using this process, antibody coated microparticles were assembled on substrates and used as capture patterns for the creation of complex cell networks. This new technology may have numerous applications in biology, e.g. for fast cell imaging, cell-cell interactions studies, or construction of cell arrays.

## 1. Introduction

Capillary assembly [1-3] is a powerful technique to deposit onto a structured surface micro or nano-objects that are initially suspended in a liquid. This process was shown to be compatible with a large range of particle sizes, from several micrometers down to 2 nm [4]. Typical experiments involve the dragging of a colloidal suspension along a surface topographically patterned with cavities or obstacles. Usually, the surface presents a partial wetting behaviour locally modified by the patterns.

The assembly mechanism that drives particle deposition is based on the interplay between drag forces induced by the fluid open surface at the vicinity of the meniscus (the orientation of which depends on the recessing wetting angle) and the confinement forces created by the protruding or recessed structures on the surface [3]. When the confinement forces induced by the capture patterns are sufficient to compensate for drag forces that push the particles towards the bulk suspension, immobilization conditions are reached. The particles are selectively trapped into the recessed or protruding structures, while they are carried away on the flat areas where no deposition occurs. As already demonstrated in previous work [3], the contact angle must be carefully adjusted to induce an efficient particles immobilization into the capture patterns. If the angle is too low, the horizontal component of the drag force is not sufficient to drag the particles over the surface. This results in a non-localized deposition of particles, which can be used eventually to create 2D arrangements of closely packed particles [5–8]. This mechanism corresponds to convective assembly. If the angle is too high, the vertical confinement induced by the meniscus is not sufficient to stabilize the particles while the contact line passes the structured substrate. As a result, the particles are carried away by the meniscus. In intermediate operating conditions, the vertical confinement force exerted by the meniscus can be efficiently exploited to induce particle immobilization in a capture pattern. In most experiments reported in the literature, the contact angle value is usually set between 30° and 60° by tuning the concentration of surfactants [3]. When conveniently controlled, this process, called capillary assembly, allows for the creation of dense or sparse arrays of particles over large areas. Both the shape and the dimensions of the capture patterns have to be chosen according to the particle size, in order to provide efficient immobilization and controlled positioning.

<sup>a</sup> Institut Curie, PSL Research University, UMR 168, Paris, F-75248, France

Centre National de la Recherche Scientifique, Université Pierre et Marie Curie Tel: +33 (0)1 56 24 67 52;

E-mail: fddelap@gmail.com; jean-louis.viovy@curie.fr

<sup>b</sup> Current affiliation: CNRS, LAAS, 7 avenue du colonel Roche, F-31400 Toulouse, France

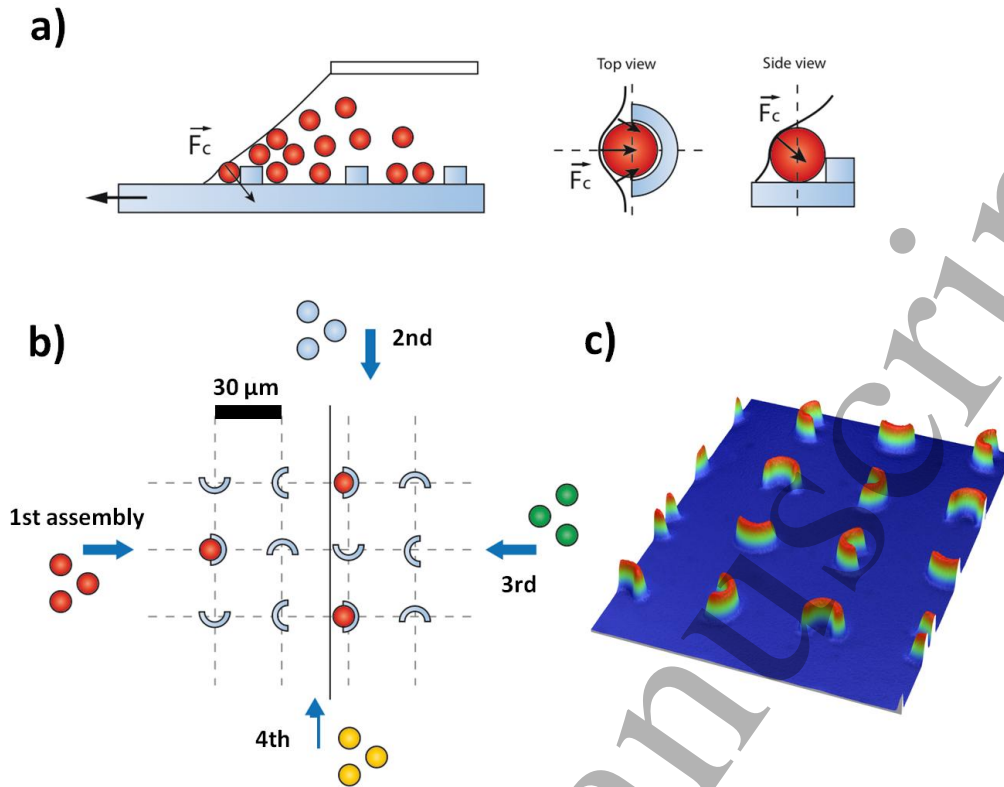


**Figure 1.** (a) Capillary assembly principle. A colloidal suspension is dragged over a surface patterned with crescent-shaped structures. Beads are carried away on flat surface by the capillary force  $F_c$ , but are selectively trapped in recessed areas or protruding obstacles. Both the lateral and vertical confinement forces control the capture efficiency and the in-plane positions of the particles. (b) Principle of multiplexed capillary assembly. Particles are only trapped when they are coming in contact with the structure by its aperture. (c) Optical profilometer image of a patterned PDMS substrate. The distance between two structures is 30  $\mu\text{m}$ . The structure height is 2  $\mu\text{m}$ .

The present work has two objectives: First, we show that it is possible to exploit the capture selectivity regarding obstacles size, geometry and orientation relative to the meniscus direction, to sequentially immobilized different types of particles on the same capture substrate, i.e. to perform a multiplexed assembly. The working principle of the multiplexed capture process is described in figure 1: four imbricated arrays of crescent-shaped patterns with four different orientations were integrated on the substrate. When capillary assembly is performed, only the patterns with their aperture facing the meniscus behave as efficient geometrical traps. Particles that arrive at patterns from any other directions are not immobilized, since the horizontal component of the steric interaction between the particle and the obstacle pushes the former away from the latter, along an escape trajectory. By taking advantage of this phenomenon, a multiplexed assembly becomes possible.

Second, we show that the assembly process, which preserves the functionality of the immobilized particles, can be used for the selective targeting and capture of cells. Precisely localizing aggregates or individual cells may have various important applications in cell-cell interaction studies, single cell behaviour observation or to build artificial cell assemblies and tissues. Several techniques have already been tested to achieve this goal, such as laser pulses [9], microwaves [10], micro contact printing [11], capillary assembly [12], dielectrophoresis [13], microwells [14], chemical surface patterning [15–19], or physical traps [20–26]... These methods have been successfully applied to the local assembly of bacteria [11, 27], yeasts [12] or mammal cells [28, 29]. However, these techniques usually require complex and expensive processes or devices and the final patterned surface dimensions are limited. Most of them are intrinsically slow because of their sequential nature, and the control of the number of cells and the deposition of different types of cells on the same area in a deterministic and precise way, i.e. multiplexed biopatterning, remain challenges. We suggest here a new way to achieve this goal by performing multiplexed assembly of beads functionalized with specific ligands. We will show that it is possible to exploit this process to generate high density arrays of functionalized particles to trap different types of cells, and thus to create multiplexed cell arrays. Actually, we suggest here a new physical traps technique extremely simple to use and able to pattern millimetric surface with thousands of cells. Most

of the physical traps techniques are using traps localized in channels. Thus the surface that can be patterned is limited by the number and sizes of the channels and the number of cell types that can be deterministically pattern in the same channel is usually limited to two, by reversing the flow in the channels and trapping cells in the two successive directions of the flow [25, 26]. Our technique is not using any channels, thus the patterned surface can be dramatically increased. Moreover, the flow can come from more than two directions allowing the patterning of more than two (here four) different types of beads and potentially, if these particles are functionalized, the building of complex cells structure.

## 2. Experimental section

### A Mold fabrication

For this study, patterned substrates (figure 1c) were prepared by casting polydimethylsiloxane (PDMS) (Dow Corning, Sylgard 184) on SU-8 2002 patterned structures obtained by photolithography on silicon wafers. Layers of SU-8 2002 negative resist were first spin coated at 3000 rpm during 30 s and further exposed on a MJB3 Karl Suss mask aligner. The resulting mold was oxidized through a 20 s air plasma treatment (Harrick PDC-32G) and then silanized with trimethylchlorosilane (TMCS) using a vapor phase deposition process performed at 100 mbar in a desiccator. The obtained structures height was  $2\pm 0.5$   $\mu\text{m}$ .

### B Substrate fabrication

PDMS (Sylgard 184) was prepared by mixing one volume of curing agent with ten volumes of base material. After degassing, the mixture was casted on the silicon wafer and cured overnight at 65 °C.

### C Particle suspensions

Experiments devoted to cell capture were performed using Epithelial Enrich dynabeads (anti-Epcam) and anti-CD3 dynabeads 4.5  $\mu\text{m}$  particles (Lifetechnology).

Proof of concept of multiplexed assembly were obtained by patterning the capture surface with i) 4.5  $\mu\text{m}$  magnetic Dynabeads, ii) 4  $\mu\text{m}$  (latex) spherical particles (FluoSpheres® Sulfate Microspheres and Epoxy/sulfate white microspheres) with different dyes (white, yellow, pink) and iii) 6  $\mu\text{m}$  Polybeads® polystyrene (PS) particles (black, blue, red, yellow).

### D Contact angle control

To control the contact angle, surfactants were added to the colloidal suspension. One volume of 10 mM sodium dodecylsulfate aqueous solution (SDS) was mixed with one volume of 0.1 % Triton X45 aqueous solution (w/v). The resulting solution was added (concentration is given in volume) to the particle suspension to control the wetting properties, and in particular the receding contact angle. Contact angle was adjusted through surfactant concentration for each particle suspension in order to maximize the efficiency of the process (yield, cleanness of the surface...). For 6  $\mu\text{m}$  PS particles (and thus the yield study), to be in the same conditions for all experiments, the volume of surfactant was systematically set to 5 % (v/v).

### E Assembly process

The setup used in this study is similar to the one previously reported by authors for capillary and convective assembly studies [3]. The PDMS templates were mounted on a motorized translation stage (PI M-410DG). A defined volume (100-200  $\mu\text{L}$ ) of microparticles suspension was then injected between the moving substrate and a tilted glass slide (tilt angle around 5°) fixed above the substrate in contact with the liquid and close to the surface (0.2-1 mm). The substrate was moved at velocities ranging from 5 to 50  $\mu\text{m/s}$ , while the drop was kept stationary by the capillary confinement effect induced by the fixed glass slide placed above the substrate. The speed was adapted empirically for each beads suspension. Temperature was controlled using a thermoelectric module located underneath the sample. The entire setup was mounted on the stage of an upright optical microscope to provide direct observation of the assembly process. The system was driven using a computer interface based on LabView (National Instruments™). In order to improve the adhesion between the beads and the substrate, the sample was air dried after each assembly step. We did not notice a significant influence of this process on the particle functionality.

### F Yield and selectivity estimation

To evaluate assembly yield, 6  $\mu\text{m}$  PS beads were used and the following parameters were set as follows. Temperature:  $T=25\text{ }^\circ\text{C}$ . Surfactant volume ratio:  $c_s=5\%$  (v/v). Assembly speed:  $v=5\text{ }\mu\text{m/s}$ . Beads concentration:  $c_B=0.27\%$  (solid content). It is interesting to notice that as the particles are dragged during the process by the meniscus, they are considerably concentrated in its vicinity. The initial concentration is not a critical parameter. Thus, the beads concentration of the suspension that is used could be reduced if necessary. A rounded corner-shape structure was chosen (see ESI “traps shape” figure). The substrate was imaged between each step with white light illumination in an inverted configuration, and the capture sites and their content were observed. The percentage of errors was defined as the number of particles trapped in “wrong” traps (sites with their opening not oriented towards incoming meniscus) over the total number of wrong sites. Similarly, an estimation of total yield of correct capture after the four assemblies was calculated as the ratio between the numbers of correct captures to the total number of traps.

### G Cells capture experiments

Two types of cancer cell lines were used: Human Ovarian Carcinoma cells (Ovcar) and Leukemia cells (Jurkat). These cells express significant levels of EpCAM and CD3 antigens on their membrane and thus can be captured with anti-EpCAM and anti-CD3 particles, respectively. Cell lines were grown in DMEM or RPMI (with 10 % of heat-inactivated fetal bovine serum, 2 mM of L-glutamine, 100 U/mL of penicillin and 100  $\mu\text{g/mL}$  of streptomycin) at  $37^\circ\text{C}$  in wet atmosphere with a controlled  $\text{CO}_2$  level of 5 %. Cells were centrifuged at 1000 rpm and resuspended in Phosphate Buffered Saline (PBS) with 1 % of Bovine Serum Albumin (BSA). The cell suspensions were incubated on the surface and washed several times in buffer to remove unbound cells. For fluorescence imaging, Jurkat cells were stained with Wheat germ agglutinine, Oregon Green® 488 conjugate and Ovcar cells were stained with Hoechst™ 33342 trihydrochloridetrihydrate.

## 3. Results and discussion

### A Design optimization

We considered patterns with four different orientations and performed a series of capillary assembly steps on the same capture substrate (see ESI movie “Beads capture”). Before each assembly step the substrate was rotated by  $90^\circ$ , allowing to specifically address a different pattern orientation. Thus by repeating the capillary assembly process in the 4 directions, it is possible to sequentially assemble 4 different populations of particles in a deterministic way. We investigated arrays of 3D protruding crescent-shaped structures (see ESI “traps shape” figure) on patterned PDMS samples. In comparison with recessed patterns, structures that extend above the substrate surface offer more flexibility and selectivity regarding the pattern orientation. The pattern lattice comprised 4 hexagonal imbricated arrays, each of them made of patterns with a specific orientation ( $0^\circ$ ,  $90^\circ$ ,  $180^\circ$ ,  $270^\circ$ ). The distance between structures was set to 30  $\mu\text{m}$ . In order to optimize capture efficiency and avoid multiple captures, the trap opening has a diameter close to the size of the particles. The inner dimensions of the traps were set to 4.9-5  $\mu\text{m}$  to enable the capture of 4 and 4.5  $\mu\text{m}$  beads and 7.2-7.55  $\mu\text{m}$  for the capture of 6  $\mu\text{m}$  beads. The height of the structures was set to  $2\pm 0.5\text{ }\mu\text{m}$ .

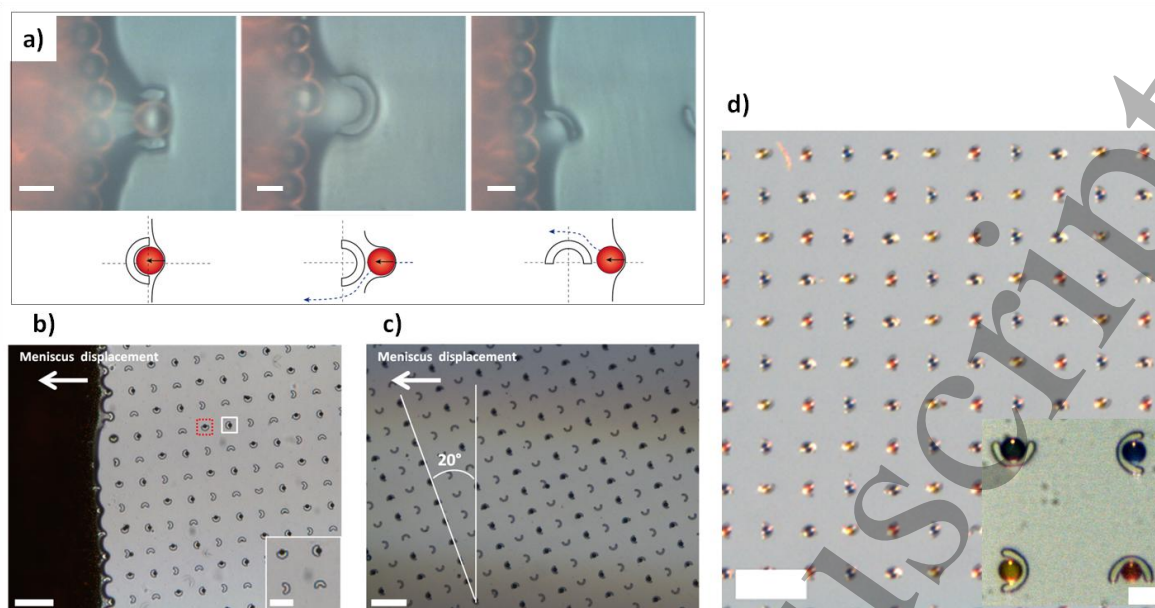


**Figure 2.** (a) Left: a structure with an aperture oriented in the direction of the meniscus captures a particle. Middle and right: A structure not oriented in the direction of the meniscus does not provide a stable position for capture (scale bar: 5  $\mu\text{m}$ ). (b) An array of 4.5  $\mu\text{m}$  particles created during the second assembly step. The trap framed with red dashed line was filled during the first assembly. The trap framed with white continuous line was filled during the second assembly (scale bar: 50  $\mu\text{m}$ ). In the corner: a zoom (scale bar: 20  $\mu\text{m}$ ). (c) An array of 6  $\mu\text{m}$  particles created if the angle between the meniscus and the aperture is 20° (the angle between the aperture and the meniscus advancement axis is thus equal to 70°). Particles are selectively trapped in two types of pattern orientation (scale bar: 50  $\mu\text{m}$ ). (d) Four different imbricated arrays of 6  $\mu\text{m}$  stained particles on PDMS (scale bar: 50  $\mu\text{m}$ ). In the corner: detailed image showing the position of the particles in the traps (scale bar: 10  $\mu\text{m}$ ).

### B Selectivity regarding pattern orientation and dimension

During capillary assembly, only the patterns with their aperture facing the meniscus provide sufficient confinement forces to induce an effective immobilization of the particles. Particles approaching obstacles with a different orientation do not reach a stable position and finally roll on the wall of the structures and bypass them without being immobilized (figure 2a). In order to investigate the selectivity of the assembly process relative to the pattern design and orientation, and thus robustness towards orientation misalignments, experiments were done with a substrate orientation relative to the meniscus varying between 0 and 90°. We found that for angles between the aperture and the direction of advancement of the meniscus comprised between 0 and 70°, on both sides since the pattern is symmetric, the capture selectivity is impeded, i.e. particles can be simultaneously immobilized into two arrays (figure 2c). Therefore, in order to trap particles in a single family of traps during each assembly, the directions of trap apertures must differ by more than 70°. Thus, in order to keep a security margin of 5° towards misalignment or minor variations in traps shapes, for these particles with these traps, only 4 different directions can be used for multiplexing, corresponding to an angle of 90° between aperture axes.

### C Multiplexed particles arrays

We performed a series of capillary assemblies, rotating the sample by 90° before each deposition. By this process, four different types of microparticles could be selectively trapped in the corresponding structures. Three difficulties must be solved to perform assemblies in series: first, the new incoming particles must be selectively trapped into the targeted structures and the assembly yield should not be impeded by the previously immobilized particles. Secondly, these new incoming particles must not be trapped on the new structures composed of a particle in its trap. Thirdly, particles previously trapped must remain stable while another assembly step is performed. The first difficulty was solved by a proper selection of traps geometry and spacing, ensuring that the shape of a contact line in the immediate vicinity of a trap is only weakly perturbed by neighbouring traps. Concerning the second problem, as previously said, only the structures with their aperture facing the meniscus are efficient traps. In other



words, only the concave part of a pattern is able to trap the particles. A convex structure does not provide a sufficient geometrical confinement to balance the capillary forces exerted by the liquid meniscus and offer a stable particle positioning. It is important to notice that the depth of the aperture of the traps has the same order of magnitude as the radius of the particles. Thus, a part of the particles protrudes from the aperture of the trap: the concave aperture is replaced by a convex, round, structure on which particles cannot be immobilized. At the junction of the particle and the inner part of the trap, a small corner is created. Nevertheless, this little concavity is too small compared to the diameter of the beads to induce a lateral confinement and lead to an efficient capture. The last difficulty was overcome by drying the surface after each deposition, in order to reinforce particles adhesion to the substrate. Indeed, upon dehydration, an intimate contact is promoted between the surface of PDMS and the particles. The origin of this intimate contact may be the deformation capabilities of PDMS or the presence of free silicone chains in the PDMS that can migrate to the surface. Figure 2b shows the second assembly of 4.5  $\mu\text{m}$  particles at 50  $\mu\text{m}/\text{s}$  with a surfactant concentration of 20 % (v/v): The particles captured during first assembly are visible in traps oriented at 90°. For 6  $\mu\text{m}$  polystyrene particles, using surfactant proportion of 5 %, 2  $\mu\text{m}$  high obstacles and a meniscus speed of 5  $\mu\text{m}/\text{s}$  during each step, the percentage of release was around one percent. Figure 2d shows the result obtained at the end of the fourth assembly with these parameters. The mean yield of correct capture of unique particles was  $94.2 \pm 3.5$  %. Accepting the possibility of multiple particles with the same functionality in the same trap (which does not alter the performance regarding the next step, see below) the mean yield was  $97.3 \pm 2.3$  %, and the mean percentage of errors was  $3.7 \pm 2.5$  %. The total correct yield at the end of the fourth assembly was estimated to  $91.6 \pm 1$  %. Thus, less than 10 % traps were empty or filled with the wrong beads.

#### D Multiplexed cells arrays

The particle assemblies obtained with this technique were used to build multiplexed cells array. The principle is described on figure 3a. A substrate patterned with two types of 4.5  $\mu\text{m}$  particles, coated with antibodies directed to Ovar and Jurkat cells, respectively, was first prepared. Ovar and Jurkat cells were then sequentially incubated on the substrate in a PBS buffer (BSA 1 %). After cells sedimentation and incubation (5 min), the substrate was rinsed in PBS. During all experiments, a layer of liquid was

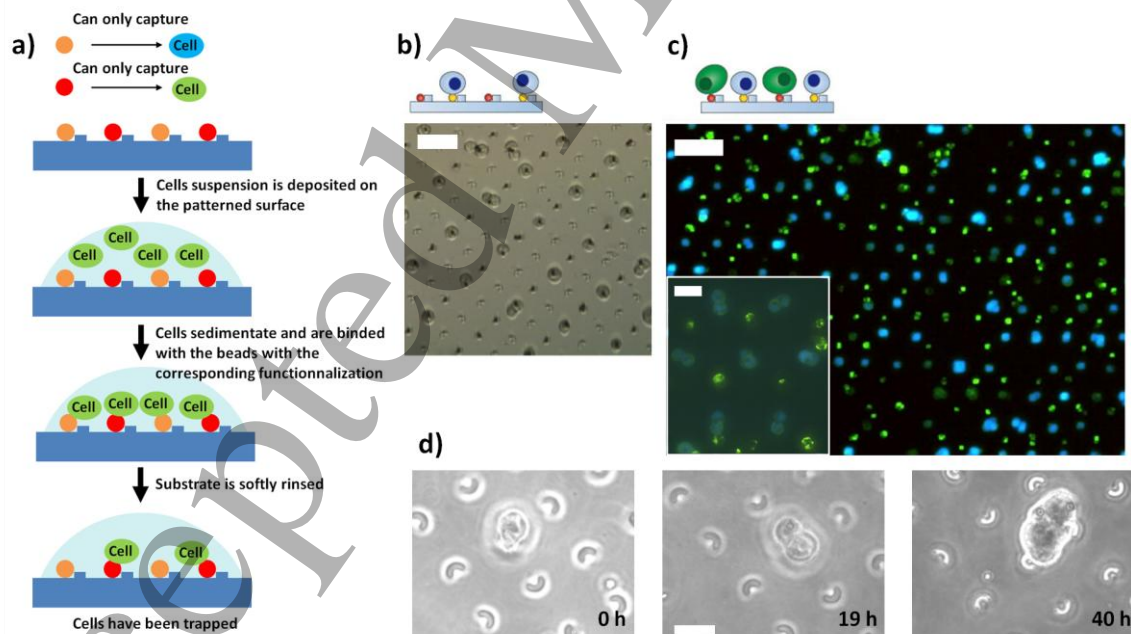


**Figure 3.** (a) Principle for the preparation of multiplexed cell arrays: A cell suspension is deposited on a surface patterned with different types of antibody-coated beads. Cells sediment on the surface and are selectively captured on the particles with the antibodies complementary to their surface antigens. Then the substrate is washed and another cell suspension is introduced. The process can be repeated several times to capture several kinds of cells. (b) On a substrate patterned with two types of antibody-coated beads, Ovar cells have been selectively trapped on 4.5  $\mu\text{m}$  particles, thus creating an hexagonal cells network. In this specific assembly, one bead over two, located in one capture site over four, arranged in an hexagonal superlattice, is expected to trap cells. The capture yield is above 87 %. (scale bar: 50  $\mu\text{m}$ ). (c) Fluorescence image of an array of stained Jurkat (green) and Ovar (blue) cells obtained after incubation (scale bar: 100  $\mu\text{m}$ ). Colors have been enhanced for clarity. A zoom is provided in the lower left corner (scale bar: 25  $\mu\text{m}$ ). (d) Here, we observe the multiplication of an Ovar cell captured on a bead into a cluster during 40 h (scale bar: 20  $\mu\text{m}$ ).



1  
2  
3 kept over the surface to avoid dehydration of the cells. To avoid the cells of one type to impede the  
4 contact of the other type of cells with the beads, we introduced the two types of cells, one after another.  
5 An image of the captured cells on the array, after one step of capture, is provided in figure 3b. In figure  
6 3c the same array is displayed after a second step of assembly (Ovcar cells are stained in blue, Jurkat  
7 ones in green). The obtained cell density is above 250 cells/mm<sup>2</sup> of each type. This shows that the  
8 surfactants used for assembly, and the drying steps used to immobilize the beads do not affect  
9 significantly the functionality of antibodies. The accuracy of cells positioning is limited by the size of  
10 the particles, i.e.  $\pm 4 \mu\text{m}$ . Finally we observed (figure 3d) the successful division of Ovcar cells trapped  
11 on a bead, showing that the trapping process is applicable for further cell studies.  
12

#### 13 14 15 **4. Conclusions**

16 Capillary assembly upon asymmetrical obstacles allows the easy and automated deposition of different  
17 types of beads (here, up to 4) in interspersed arrays. Using particles functionalized with different  
18 antibodies, these bead arrays can subsequently be used as a substrate for the intersperse assembly of  
19 large arrays of cells of different types, including mammal cells.

20 Cells have been captured with high yield and selectivity on their respective antibodies coated particles,  
21 creating two hexagonal imbricated cells networks corresponding to the hexagonal organization of the  
22 PDMS structures prepared on the substrate. At the assembly velocities used here, several square  
23 millimetres can be covered with beads in a few minutes. The cells assembly itself also takes around 5  
24 min for each cell type, so regular arrays of typically 10 000 individual cell spots can be prepared in less  
25 than one hour, making the method simple, versatile and high throughput. We used here a very simple  
26 regular array, but the method can be extended to almost any arbitrary arrangement with a micrometric  
27 resolution. Moreover, once captured, the cells remain viable for culture or any further molecular  
28 characterization. We are thus convinced that the low cost, effectiveness, and above all easiness, of this  
29 cell patterning approach is an enabling tool to develop simple and high-throughput screening  
30 technologies for cell assays or cell-cell interactions studies.  
31

#### 32 33 **Acknowledgements**

34 This work was supported by a fellowship to V. Taniga from ANR project REDLOC, by ERC AdG  
35 project Cello, by the INCA/DHOS "recherche translationnelle" program, by Investissement d'avenir  
36 ANR project "Digidiag", and by Nadine and Diatools European Projects (FP7).  
37

#### 38 39 40 **Notes and references**

- 41  
42 [1] Y. Yin, Y. Lu, B. Gates, and Y. Xia, "Template-assisted self-assembly: a practical route to complex  
43 aggregates of monodispersed colloids with well-defined sizes, shapes, and structures," *J. Am. Chem. Soc.*,  
44 vol. 123, no. 36, pp. 8718–8729, 2001.
- 45 [2] F. Juillerat, H. H. Solak, P. Bowen, and H. Hofmann, "Fabrication of large-area ordered arrays of  
46 nanoparticles on patterned substrates," *Nanotechnology*, vol. 16, no. 8, pp. 1311–1316, 2005.
- 47 [3] L. Malaquin, T. Kraus, H. Schmid, E. Delamarche, and H. Wolf, "Controlled particle placement through  
48 convective and capillary assembly," *Langmuir*, vol. 23, no. 23, pp. 11513–11521, Nov. 2007.
- 49 [4] Y. Cui, M. T. Björk, J. A. Liddle, C. Sönnichsen, B. Boussert, and A. P. Alivisatos, "Integration of  
50 Colloidal Nanocrystals into Lithographically Patterned Devices," *Nano Lett.*, vol. 4, no. 6, pp. 1093–  
51 1098, Jun. 2004.
- 52 [5] N. D. Denkov, O. D. Velev, P. A. Kralchevsky, I. B. Ivanov, H. Yoshimura, and K. Nagayama, "Two-  
53 dimensional crystallization," *Nature*, vol. 361, no. 6407, pp. 26–26, Jan. 1993.
- 54 [6] E. Adachi, A. Dimitrov, and K. Nagayama, "Stripe patterns formed on a glass surface during droplet  
55 evaporation," *Langmuir*, vol. 11, pp. 1057–1060, 1995.
- 56 [7] A. S. Dimitrov and K. Nagayama, "Continuous convective assembling of fine particles into two-  
57 dimensional arrays on solid surfaces," *Langmuir*, vol. 12, no. 5, pp. 1303–1311, Jan. 1996.
- 58 [8] B. Prevo and O. D. Velev, "Controlled, rapid deposition of structured coatings from micro-and  
59 nanoparticle suspensions," *Langmuir*, vol. 20, no. 6, pp. 2099–2107, 2004.  
60

- 1  
2  
3 [9] J. A. Barron, P. Wu, H. D. Ladouceur, and B. R. Ringeisen, "Biological laser printing: a novel technique  
4 for creating heterogeneous 3-dimensional cell patterns.," *Biomed. Microdevices*, vol. 6, no. 2, pp. 139–  
5 47, Jun. 2004.
- 6 [10] F. Guo, P. Li, J. B. French, Z. Mao, H. Zhao, S. Li, N. Nama, J. R. Fick, S. J. Benkovic, and T. J. Huang,  
7 "Controlling cell-cell interactions using surface acoustic waves.," *Proc. Natl. Acad. Sci. U. S. A.*, vol.  
8 112, no. 1, pp. 43–8, 2015.
- 9 [11] L. Xu, L. Robert, Q. Ouyang, F. Taddei, Y. Chen, A. B. Lindner, and D. Baigl, "Microcontact printing of  
10 living bacteria arrays with cellular resolution.," *Nano Lett.*, vol. 7, no. 7, pp. 2068–72, Jul. 2007.
- 11 [12] M. C. Park, J. Y. Hur, K. W. Kwon, S. H. Park, and K. Y. Suh, "Pumpless, selective docking of yeast  
12 cells inside a microfluidic channel induced by receding meniscus.," *Lab Chip*, vol. 6, no. 8, pp. 988–994,  
13 2006.
- 14 [13] B. M. Taff and J. Voldman, "A scalable addressable positive-dielectrophoretic cell-sorting array.," *Anal.*  
15 *Chem.*, vol. 77, no. 24, pp. 7976–83, Dec. 2005.
- 16 [14] M. Charnley, M. Textor, A. Khademhosseini, and M. P. Lutolf, "Integration column: microwell arrays  
17 for mammalian cell culture.," *Integr. Biol. (Camb)*, vol. 1, no. 11–12, pp. 625–34, Dec. 2009.
- 18 [15] R. S. Kane, S. Takayama, E. Ostuni, D. E. Ingber, and G. M. Whitesides, "Patterning proteins and cells  
19 using soft lithography.," *Biomaterials*, vol. 20, no. 23–24, pp. 2363–76, Dec. 1999.
- 20 [16] J. Nakanishi, T. Takarada, K. Yamaguchi, and M. Maeda, "Recent advances in cell micropatterning  
21 techniques for bioanalytical and biomedical sciences.," *Anal. Sci.*, vol. 24, no. 1, pp. 67–72, Jan. 2008.
- 22 [17] A. Cerf, J.-C. Cau, and C. Vieu, "Controlled assembly of bacteria on chemical patterns using soft  
23 lithography.," *Colloids Surf. B. Biointerfaces*, vol. 65, no. 2, pp. 285–91, Oct. 2008.
- 24 [18] J. M. Collins and S. Nettikadan, "Subcellular scaled multiplexed protein patterns for single cell  
25 cocultures.," *Anal. Biochem.*, vol. 419, no. 2, pp. 339–341, 2011.
- 26 [19] J. M. Collins, R. T. S. Lam, Z. Yang, B. Semsarieh, A. B. Smetana, and S. Nettikadan, "Targeted  
27 delivery to single cells in precisely controlled microenvironments.," *Lab Chip*, vol. 12, no. 15, pp. 2643–  
28 8, 2012.
- 29 [20] J. Nilsson, M. Evander, B. Hammarström, and T. Laurell, "Review of cell and particle trapping in  
30 microfluidic systems.," *Anal. Chim. Acta*, vol. 649, no. 2, pp. 141–57, Sep. 2009.
- 31 [21] D. Di Carlo, L. Y. Wu, and L. P. Lee, "Dynamic single cell culture array.," *Lab Chip*, vol. 6, no. 11, pp.  
32 1445–9, Nov. 2006.
- 33 [22] R. Burger, D. Kurzbuch, R. Gorkin, G. Kijanka, M. Glynn, C. McDonagh, and J. Ducrée, "An integrated  
34 centrifugo-opto-microfluidic platform for arraying, analysis, identification and manipulation of  
35 individual cells.," *Lab Chip*, Nov. 2014.
- 36 [23] A. M. Skelley, O. Kirak, H. Suh, R. Jaenisch, and J. Voldman, "Microfluidic control of cell pairing and  
37 fusion.," *Nat. Methods*, vol. 6, no. 2, pp. 147–52, Feb. 2009.
- 38 [24] S. Suri, A. Singh, A. H. Nguyen, A. M. Bratt-Leal, T. C. McDevitt, and H. Lu, "Microfluidic-based  
39 patterning of embryonic stem cells for in vitro development studies.," *Lab Chip*, vol. 13, no. 23, pp.  
40 4617–4624, 2013.
- 41 [25] L. Lin, Y.-S. Chu, J. P. Thiery, C. T. Lim, and I. Rodriguez, "Microfluidic cell trap array for controlled  
42 positioning of single cells on adhesive micropatterns.," *Lab Chip*, vol. 13, no. 4, pp. 714–21, Feb. 2013.
- 43 [26] K. Zhang, C.-K. Chou, X. Xia, M.-C. Hung, and L. Qin, "Block-Cell-Printing for live single-cell  
44 printing.," *Proc. Natl. Acad. Sci.*, vol. 111, no. 8, pp. 2948–2953, 2014.
- 45 [27] S. A scalable addressable positive-dielectrophoretic cell-sorting array. Rozhok, Z. Fan, D. Nyamjav, C.  
46 Liu, C. A. Mirkin, and R. C. Holz, "Attachment of motile bacterial cells to prealigned holed  
47 microarrays.," *Langmuir*, vol. 22, no. 26, pp. 11251–4, Dec. 2006.
- 48 [28] A. Azioune, M. Storch, M. Bornens, M. Théry, and M. Piel, "Simple and rapid process for single cell  
49 micro-patterning.," *Lab Chip*, vol. 9, no. 11, pp. 1640–2, Jun. 2009.
- 50 [29] V. Sivagnanam, B. Song, C. Vandevyver, J.-C. G. Bünzli, and M. A. M. Gijs, "Selective breast cancer  
51 cell capture, culture, and immunocytochemical analysis using self-assembled magnetic bead patterns in a  
52 microfluidic chip.," *Langmuir*, vol. 26, no. 9, pp. 6091–6, May 2010.
- 53  
54  
55  
56  
57  
58  
59  
60